Thermodynamics and kinetics of order-disorder processes derived from the cluster-activation method and microscopic diffusion theory

Long-Qing Chen
Department of Materials Science and Engineering, Pennsylvania State University, University Park, Pennsylvania 16802
(Received 26 July 1993; revised manuscript received 4 November 1993)

The thermodynamics and kinetics of order-disorder processes derived from the cluster-activation method (CAM) and microscopic diffusion theory (MDT) are examined. In the single-site approximation, the homogeneous long-range-order kinetic equations for the direct exchange mechanism (Kawasaki dynamics) in the CAM are derived by employing a kinetic theory of a Markovian nature whereas the kinetic equations in MDT are derived from the Onsager-type diffusion equations based on a microscopic mean-field free-energy functional. While the single-site approximation in MDT results in equilibrium states corresponding to the Bragg-Williams approximation, the same approximation in the CAM produces equilibrium states close to the Bethe (nearest-neighbor-pair) approximation. The physical origin underlying the partial inclusion of nearest-neighbor-pair correlation information in the single-site approximation of the CAM is discussed. It is shown that if the values of (ordering energy)/k_BT and the time-dependent long-range parameter η are small ($\ll 1$), the kinetic equations in the CAM reduce to those in MDT. It is demonstrated that the disordering kinetics obtained from the linearized equations for both models agree, at least qualitatively, with those from nonlinear equations but not the ordering kinetics.

I. INTRODUCTION

Various theoretical models of order-disorder have been proposed in the literature and the corresponding kinetic equations have been extensively employed in the study of ordering and disordering kinetics in alloys. There are generally two types of kinetic models. One assumes the existence of a free-energy functional which is a function of order parameters and their rates of change with respect to time are assumed to be linearly proportional to the thermodynamic driving force. For example, the continuum time-dependent-Ginzburg-Landau (TDGL) or Allen-Cahn (AC) kinetic equations[1] belong to this type. Excellent reviews exist for the various applications of this type of kinetic equations.[2] Recently, there have also been extensive applications of Onsager-type kinetic equations from a microscopic diffusion theory (MDT) which is also based on a free-energy functional.[3,4] The other type of kinetic model, which is uniquely different from the free-energy-functional-based model, is that derived from microscopic kinetic master equations.[5] The kinetic equations in this type of model are written with respect to a one-, two-, or n-particle cluster (where n is the number of particles in a given cluster) correlation functions, and their rates of change are highly nonlinear functions of the thermodynamic driving force. There is no free-energy functional required in deriving the kinetic equations. Therefore, this type of model will be called the cluster-activation method (CAM) in this paper. Both short- and long-range-order kinetics have been studied based on this type of kinetic model.[6-15] The main purpose of this paper is to give a critical examination of MDT (or TDGL or AC) and CAM. The plan of the paper is as follows: the kinetic equations from the two distinctly different models, MDT and CAM, are given in Sec. II; the equilibrium solutions to the kinetic equations are compared in Sec. III; Sec. IV presents the results on ordering kinetics and the results on disordering kinetics; Sec. V derived the linearized version of the kinetic equations, and the ordering and disordering kinetics obtained from the linear and nonlinear equations are compared; the major differences between these two types of kinetic models are discussed in Sec. VI; and, finally, the major findings of this paper are summarized in Sec. VII.

II. KINETIC EQUATIONS

A. Long-range-order kinetic equation derived from MDT

In MDT, the atomic structure and morphologies of a binary alloy (A-B) are described by single-site occupation probability functions, $P_A(\mathbf{r},t)$, defined at lattice site $\mathbf{r}$ for a given time t. It is assumed that there exists a free-energy functional that can describe both equilibrium and nonequilibrium states of a system even though free energy is only defined for equilibrium states. The evolution of a nonequilibrium distribution of the single-site occupating probability function towards equilibrium is described by the Onsager-type diffusion equations in which the rate of change of the single-site occupation probability function is linearly proportional to the thermodynamic driving force which is defined as the variation derivative of the total free energy with respect to the single-site occupation probability function,[4] i.e.,

$$\frac{dP_A(\mathbf{r},t)}{dt}=\sum_{\mathbf{r}'}\frac{c(1-c)L_0(\mathbf{r}-\mathbf{r}')}{k_BT}\frac{\delta F}{\delta P_A(\mathbf{r}',t)}\ , \qquad (1)$$

where $L_0(\mathbf{r}-\mathbf{r}')$ is a probability of an elementary diffusional jump from site $\mathbf{r}$ to site $\mathbf{r}'$ per unit of time, k_B is the Boltzmann constant, T is temperature, c is the alloy

composition, t is time, and F is the Helmholtz free energy. In the single-site approximation, F is given by

$$F=\frac{1}{2}\sum_{\mathbf{r}'}\sum_{\mathbf{r}''}W(\mathbf{r}'-\mathbf{r}'')P_A(\mathbf{r}')P_A(\mathbf{r}'') +k_BT\sum_{\mathbf{r}'}\{P_A(\mathbf{r}')\ln[P_A(\mathbf{r}')] +[1-P_A(\mathbf{r}')]\ln[1-P_A(\mathbf{r}')]\} . \quad (2)$$

In a binary alloy, $W(\mathbf{r}'-\mathbf{r}'')$ is the interchange energy defined as

$$W(\mathbf{r}'-\mathbf{r}'')=V_{AA}(\mathbf{r}'-\mathbf{r}'')+V_{BB}(\mathbf{r}'-\mathbf{r}'') -2V_{AB}(\mathbf{r}'-\mathbf{r}'') , \quad (3)$$

where $V_{AA}(\mathbf{r}'-\mathbf{r}'')$, $V_{BB}(\mathbf{r}'-\mathbf{r}'')$, and $V_{AB}(\mathbf{r}'-\mathbf{r}'')$ are pairwise interaction energies of A-A, B-B, and A-B pairs of atoms located at the lattice sites $\mathbf{r}'$ and $\mathbf{r}''$, respectively.

Since we are only concerned with homogeneous long-range-order kinetics, the single-site occupation probability function, $P_A(\mathbf{r},t)$, may be expressed in terms of a long-range-order parameter and the alloy composition by employing the static concentration wave method (SCWM).[16] Let us consider a typical case of AB order with a stoichiometric composition $\frac{1}{2}$ such as the case for the $B2$ order in a bcc lattice or the case of chess-board order in a two-dimensional square lattice. For such an ordered phase, the single-site occupation probability function can be written as

$$P_A(\mathbf{r})=c+c\eta\exp(i\mathbf{k}_0\mathbf{r}) , \quad (4)$$

where c is the composition, η is the long-range-order parameter, and $\mathbf{k}_0$ is the superlattice vector for the corresponding ordered phase. Substituting (4) and (2) into (1), we have

$$\frac{d\eta}{dt}=\frac{c(1-c)L_0(\mathbf{k}_0)}{k_BT}\left[c\eta V(\mathbf{k}_0)+k_BT\ln\frac{1+\eta}{1-\eta}\right] , \quad (5)$$

where $L_0(\mathbf{k}_0)$ and $V(\mathbf{k}_0)$ are the Fourier transforms of $L_0(\mathbf{r})$ and $W(\mathbf{r})$ evaluated at $\mathbf{k}_0$, respectively. Assuming nearest-neighbor jumps only, the Fourier transform of $L_0(\mathbf{r})$ is given by

$$L_0(\mathbf{k})=-zL_1[1-\cos(\mathbf{kr})] , \quad (6)$$

where z is the number of nearest neighbors ($z=8$ for bcc and $z=4$ for square lattice) and L_1 is the probability of atom jump between nearest-neighbor sites within a time unit. Let us consider a particular case of $B2$ order in the bcc lattice. The Fourier transform of $W(\mathbf{r})$ for bcc with a nearest-neighbor interaction model is

$$V(k)=zw_1\cos(\pi h)\cos(\pi k)\cos(\pi l) , \quad (7)$$

where w_1 is the effective interchange energies between nearest-neighbor atoms and h, k, and l are defined in

$$\mathbf{k}=2\pi(h\mathbf{a}_1^*+k\mathbf{a}_2^*+l\mathbf{a}_3^*) \quad (8)$$

in which $\mathbf{a}_1^*$, $\mathbf{a}_2^*$, and $\mathbf{a}_3^*$ are the unit vectors in the reciprocal space of the bcc lattice. Substituting the superlattice vector for $B2$ order,

$$\mathbf{k}_0=2\pi(\mathbf{a}_1^*+\mathbf{a}_2^*+\mathbf{a}_3^*) \quad (9)$$

into (5), we have the long-range-order kinetic equation,

$$\frac{d\eta}{dt}=\frac{zL_1}{2}\left[\frac{z\eta w_1}{2k_BT}+\ln\left[\frac{1-\eta}{1+\eta}\right]\right] . \quad (10)$$

The same equation may be derived from the A-C kinetic model by assuming the following mean-field free-energy functional for the $B2$ ordered phase,

$$F=\frac{1}{2}V(0)c^2+\frac{1}{2}V(k_0)(c\eta)^2 +\frac{k_BT}{2}[(c+c\eta)\ln(c+c\eta)(1-c-c\eta)\ln(1-c-c\eta)+(c-c\eta)\ln(c-c\eta)+(1-c+c\eta)\ln(1-c+c\eta)] , \quad (11)$$

where $V(0)$ is the Fourier transform of $W(\mathbf{r})$ evaluated at $\mathbf{k}=0$ and $c=\frac{1}{2}$. Since we are only concerned with homogeneous order, the gradient energy term is zero in the A-C model. The kinetic equation for the long-range $B2$ order is then

$$\frac{d\eta}{dt}=-L_\eta\frac{\delta F}{\delta\eta} , \quad (12)$$

where L_η is the kinetic coefficient. By identifying L_η with

$$c(1-c)L_0(\mathbf{k}_0)/k_BT ,$$

the kinetic equation (12) is exactly the same as (10).

B. Long-range-order kinetic equation derived from CAM[5]

In CAM, the structural state of an alloy at a given temperature and pressure is described by a set of multiparticle distribution functions or cluster probabilities, $P_{\alpha_1,\ldots,\alpha_n}(\mathbf{r}_1,\ldots,\mathbf{r}_n;t)$, where t is time, $\mathbf{r}_1,\ldots,\mathbf{r}_n$ are lattice sites, and $a_1,\ldots,a_n$ are types of atoms. In order to compare the long-range-order kinetics derived from MDT and CAM, single-site approximation is also employed in CAM. In this approximation, the state of an alloy is described by the single-site probability function as in MDT. Different from MDT, the kinetic equations are written down without referring to any free-energy functionals. Moreover, there is no assumption that the rate of change of the single-site occupation probability function

with respect to time is linearly proportional to the thermodynamic driving force. Many different mechanisms for diffusion are possible, but I will assume the direct exchange mechanism often called the Kawasaki dynamics.

In the direct exchange mechanism, a pair consisting of an A atom at site $\mathbf{r}$ and a B atom at a neighboring site $\mathbf{r}+\delta$ is considered. At a given temperature and with any given set of atoms at the sites around this pair, there exists a probability that the two atoms, A and B, will directly interchange their positions. Let $\{\mathbf{x}\}$ represent the set of neighboring sites and $\{X\}$ the set of atoms on these sites. I denote $R_{AB}(\{X\})$ as the rate at which the AB pair interchanges under the influence of the set of neighboring atoms $\{X\}$. Similarly, $R_{BA}(\{X\})$ is the rate at which the BA pair will interchange under the same environment. Then the rate of change of the probability that the site $\mathbf{r}$ be occupied by an A atom is given by

$$\frac{dP_A(\mathbf{r})}{dt}=\sum_{\delta}\sum_{\{X\}}P_{BA\{X\}}(\mathbf{r},\mathbf{r}+\delta,\{x\})R_{BA}(\{X\})-\sum_{\delta}\sum_{\{X\}}P_{AB\{X\}}(\mathbf{r},\mathbf{r}+\delta,\{x\})R_{AB}(\{X\}) , \tag{13}$$

where the first and second terms on the right-hand side are the average rates at which, at site $\mathbf{r}$, A atoms are appearing and disappearing, respectively, $\sum_{\delta}$ denotes the summation over all the nearest-neighbor sites δ of $\mathbf{r}$, and

$$P_{AB\{X\}}(\mathbf{r},\mathbf{r}+\delta,\{\mathbf{x}\})$$

is the probability of finding an A atom at $\mathbf{r}$, a B atom at $\mathbf{r}+\delta$, and the set $\{X\}$ at the neighboring sites $\{\mathbf{x}\}$ simultaneously. A similar equation can be written down for $dP_B(\mathbf{r})/dt$, which is the negative of $dP_A(\mathbf{r})/dt$ since $P_A(\mathbf{r})+P_B(\mathbf{r})=1$. In principle, given an initial set of single-site distribution functions, the set of equations of motion uniquely determine the evolution of nonequilibrium states of a quenched system as a function of time.

In the single-site approximation, the distribution function (also called the cluster probability),

$$P_{AB\{X\}}(\mathbf{r},\mathbf{r}+\delta,\{\mathbf{x}\}) ,$$

can be written as

$$P_{AB\{X\}}(\mathbf{r},\mathbf{r}+\delta,\{\mathbf{x}\})=P_A(\mathbf{r})P_B(\mathbf{r}+\delta)P_x(\mathbf{x}) . \tag{14}$$

Following Vineyard, the rate constants are given by

$$R_{AB}(\{X\})=\nu\exp\left[\frac{-U}{k_BT}-\frac{\Delta E}{2k_BT}\right] ,$$
$$R_{BA}(\{X\})=\nu\exp\left[\frac{-U}{k_BT}+\frac{\Delta E}{2k_BT}\right] , \tag{15}$$

where ν is approximately the Debye vibrational frequency associated with the interchange, U is the average barrier height for the interchange, and ΔE is the energy difference between the configuration after and before the atomic exchange, $AB\rightarrow BA$, i.e.,

$$\Delta E=E_{BA}-E_{AB} , \tag{16}$$

where E_{BA} is the configuration energy after the atomic exchange and E_{AB} is the configuration energy before the exchange.

For homogeneous order, the set of kinetic equations can be reduced to a single kinetic equation for the long-range-order parameter η as in MDT. By substituting (4) and (14) into (13), the kinetic equation (13) for single-site occupating probability function is reduced to[5]

$$\frac{d\eta}{dt}=\frac{1}{2}K_0(1-\eta)^2-\frac{1}{2}K_d(1+\eta)^2 , \tag{17}$$

where K_0 and K_d, after some mathematical manipulation, are given by

$$K_0=z\nu\exp\left[-\frac{U}{k_BT}\right]\exp\left[-\frac{(z-1)w_1}{2k_BT}\right]\times\left\{1+\frac{1}{2}(1+\eta)\left[\exp\left[\frac{w_1}{2k_BT}\right]-1\right]\right\}^{2(z-1)} ,$$
$$K_0=z\nu\exp\left[-\frac{U}{k_BT}\right]\exp\left[\frac{(z-1)w_1}{2k_BT}\right]\times\left\{1+\frac{1}{2}(1+\eta)\left[\exp\left[-\frac{w_1}{2k_BT}\right]-1\right]\right\}^{2(z-1)} , \tag{18}$$

where z is the number of nearest neighbors and w_1 is the interchange energy between atoms at the nearest-neighbor sites.

III. THE EQUILIBRIUM SOLUTIONS TO THE KINETIC EQUATIONS

By definition, at equilibrium, the order of a state does not change with time. Therefore, the equilibrium solutions to the kinetic equations are obtained by setting $d\eta/dt$ equal to zero. Stable or metastable equilibrium occurs at zeros where the plot of $d\eta/dt[=f(\eta)]$ vs η has a negative slope and unstable equilibrium occurs at zeros where $f(\eta)$ has a positive slope. For both Eqs. (10) and (17), $\eta=0$ is a solution to $d\eta/dt=0$, which corresponds to the unstable disordered state when the temperature of a system is below the critical temperature for ordering. Below T_c, there is an equilibrium solution to $d\eta/dt=0$ which varies as a function of temperature. It is shown below that the dependencies of equilibrium long-range-order parameter on temperature for the two kinetic equations (10) and (17) are different in spite of the fact that the same single-site approximation is employed.

A. The equilibrium solution to kinetic equation in MDT

By setting $d\eta/dt$ in (10) equal to zero, we obtain

$$\frac{z\eta_e w_1}{2}=k_BT\ln\left[\frac{1+\eta_e}{1-\eta_e}\right] \tag{19}$$

or, writing the temperature as a function of the equilibrium long-range-order parameter η_e,

$$T=\frac{z\eta_e w_1}{2k_B \ln[(1+\eta_e)/(1-\eta_e)]} . \tag{20}$$

Expression (20) is exactly the solution that one would obtain using the Bragg-Williams approximation. The critical temperature for ordering is defined as the temperature at which $\eta_e \to 0$,

$$T_c=\frac{zw_1}{4k_B} . \tag{21}$$

B. The equilibrium solution to the kinetic equation in CAM

The equilibrium solution to Eq. (17) has been previously derived by Yamauchi,[17]

$$T=\frac{w_1}{2k_B \ln\left[\dfrac{(1+\eta_e)^{z/(z-1)}-(1-\eta_e)^{z/(z-1)}}{(1+\eta_e)(1-\eta_e)^{1/(z-1)}-(1-\eta_e)(1+\eta_e)^{1/(z-1)}}\right]} , \tag{22}$$

where z is the number of nearest neighbors.

The critical temperature is given by

$$T_c=\frac{w_1}{2k_B \ln[z/(z-2)]} , \tag{23}$$

which is, surprisingly, the same critical temperature resulted from a Bethe approximation rather than the BW critical temperature that one would expect in a single-site approximation. The temperature dependence of η_e is close to but not exactly the same as the Bethe approximation.

To compare the equilibrium solutions to the two different kinetic equations, the equilibrium long-range-order parameters η_e as a function of temperature are plotted together with the solution from the BW and Bethe approximations in Fig. 1. Figure 1 shows that results obtained from CAM are close to the Bethe approximation rather than the BW approximation. However, the equilibrium solution from MDT corresponds to exactly to the BW approximation as expected. It should be emphasized that in both cases the single-site approximation is employed. The physical origin underlying the different equilibrium states between the two different models will be discussed later in the paper.

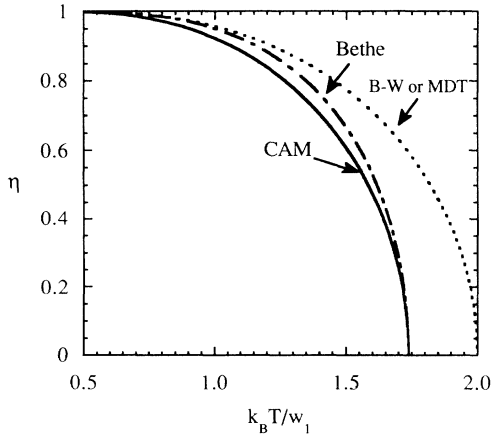

FIG. 1. Long-range-order parameter as a function of temperature. Solid line: CAM; dot-dashed line: Bethe approximation; dotted line: Bragg-Williams approximation or microscopic diffusion equation.

IV. ORDERING AND DISORDERING KINETICS

To obtain the ordering kinetics, kinetic equations are solved by the simple Euler technique,

$$\eta(t+\Delta t)=\eta(t)+\frac{d\eta}{dt}\Delta t , \tag{24}$$

where Δt is time step for integration. The following reduced times are defined:

$$t^*=\frac{tL_1}{2} \quad \text{for MDT} ,$$

$$t^*=t\nu\exp(-U/k_BT) \quad \text{for CAM} .$$

As will be shown later, these choices of reduced time units ensure that the kinetic equation in CAM reduces to that from MDT in the limit of small driving force and small long-range-order parameter values. The kinetics of ordering is demonstrated by obtaining the evolution of the long-range-order parameter as a function of the reduced time t^*. A value 0.0001 is assigned as the initial value of the long-range-order parameter in all cases. The time step for integration, Δt, is chosen to be 0.01. Since Eqs. (10) and (17) produce different critical temperatures T_c, the kinetics of ordering is compared at the same reduced temperature, T/T_c.

The values of the long-range-order parameters obtained from MDT and CAM are plotted in Fig. 2 for $T/T_c=0.5$. It is shown that ordering kinetics from the two types of kinetic models are quite different even though they are qualitatively similar. Ordering occurs at an earlier time using the kinetic equation from CAM than that obtained from MDT.

For investigating the disordering kinetics, a temperature of $T/T_c=2.0$ is selected. For all calculations, an initial value of 0.999 is assigned to the long-range-order parameter and the time step is chosen to be 0.01.

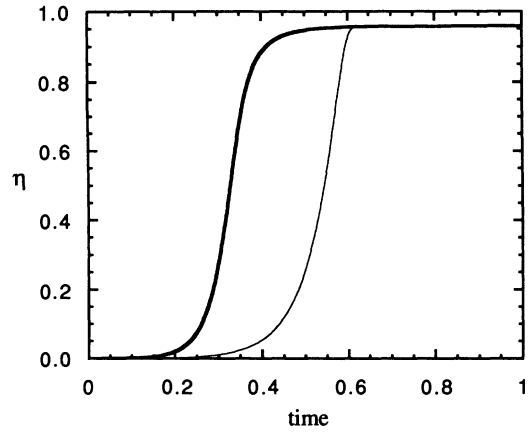

FIG. 2. The temporal evolution of long-range-order parameter as a function of time during ordering at a temperature $T/T_c=0.5$ for MDT and CAM. Thick solid line: CAM; thin solid line: MDT.

The long-range-order parameters as functions of time are plotted in Fig. 3. In contrast to the ordering kinetics, disordering occurs at an earlier time in MDT than CAM.

V. LINEARIZED KINETIC EQUATIONS

In general, the rate of change of η with respect to time is a function of $f(\eta)$, i.e.,

$$\frac{d\eta}{dt}=f(\eta)\ . \tag{25}$$

The linearized version of the kinetic equation of (25) is given by

$$\frac{d\eta}{dt}=\left.\frac{\partial f(\eta)}{\partial\eta}\right|_{\eta=\eta_e}(\eta-\eta_e)\ . \tag{26}$$

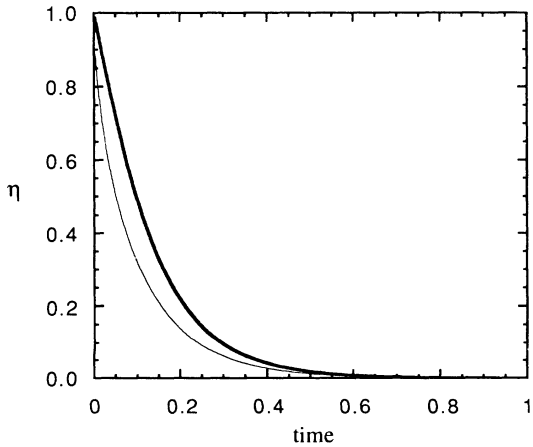

FIG. 3. The temporal evolution of long-range-order parameter as a function of time during disordering at a temperature $T/T_c=2.0$ for MDT and CAM. Thick solid line: CAM; thin solid line: MDT.

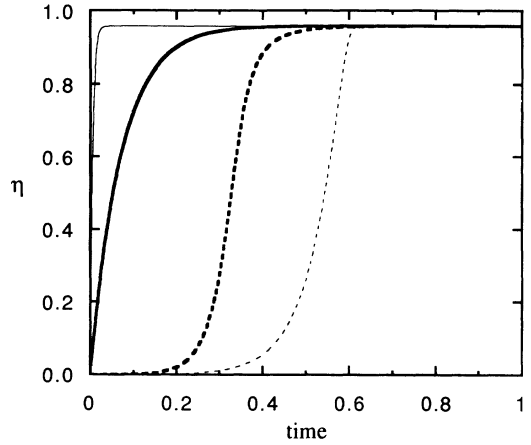

FIG. 4. A comparison of the ordering kinetics at a temperature $T/T_c=0.5$ between nonlinear and linearized kinetic equations. Thick solid line: linearized CAM equation; thin solid line: linearized MDT equation; thick dotted line: nonlinear CAM equation; thin dotted line: nonlinear MDT equation.

For MDT,

$$\left.\frac{\partial f(\eta)}{\partial\eta}\right|_{\eta=\eta_e}=\frac{zL_1}{2}\left[\frac{zw_1}{2k_BT}-\frac{2}{(1-\eta_e^2)}\right] \tag{27}$$

and for CAM,

$$\left.\frac{\partial f(\eta)}{\partial\eta}\right|_{\eta=\eta_e}=2K_0|_{\eta=\eta_e}(1-\eta_e)^2\times\left[\frac{(z-1)\gamma}{1-\eta_e^2\gamma^2}-\frac{1}{(1-\eta_e^2)}\right], \tag{28}$$

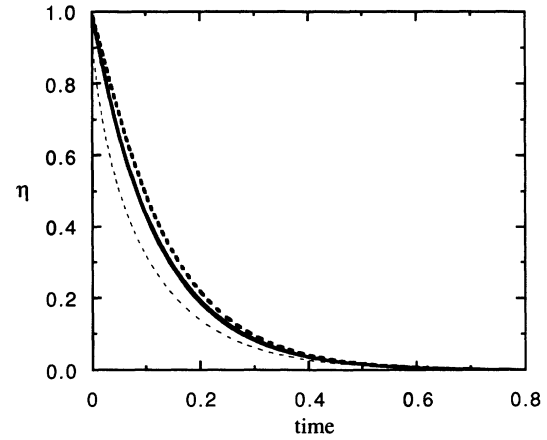

FIG. 5. A comparison of the disordering kinetics at a temperature $T/T_c=2.0$ between linearized and nonlinear kinetic equations. Thick solid line: linearized CAM equation; thin solid line: linearized MDT equation (superimposed with the solid thick line); thick dotted line: nonlinear CAM equation; thin dotted line: nonlinear MDT equation.

where

$$\gamma=\tanh(w_1/4k_BT) .$$

The ordering kinetics obtained from the linearized kinetic equations are compared with those obtained from the nonlinear equations. It is shown in Fig. 4 that in both cases the linearized equations describe very poorly the ordering kinetics for $T/T_c=0.5$. They are not even qualitatively correct. However, the disordering kinetics obtained at $T/T_c=2.0$ from linearized equations are in reasonably good agreement, at least qualitatively, with those from the nonlinear equations as shown in Fig. 5. This is particularly true for CAM.

VI. DISCUSSIONS

A. The origin for the lack of well-known equilibrium states in CAM

To understand why the kinetic equations in CAM do not produce the well-known BW or Bethe equilibrium states, let us first simplify the kinetic coefficients, K_0 and K_D, in Eq. (17) by employing two approximation formulas:

$$\exp(x)-1\approx x$$

and

$$(1+x)^n\approx\exp(nx) .$$

The simplified coefficients are

$$K_0\approx z\nu\exp\left[\left[-U\frac{(z-1)\eta w_1}{2}\right]\Big/k_BT\right] ,$$
$$K_D\approx z\nu\exp\left[\left[-U-\frac{(z-1)\eta w_1}{2}\right]\Big/k_BT\right] . \tag{29}$$

These approximations are apparently very good for $T\gg w_1/2k_B$. As a matter of fact, the equations become exact when $\eta=1$. Therefore, they remain fairly accurate for η close to equilibrium at all temperatures.

Substituting the kinetic coefficients (29) back into the kinetic equation (17), we have

$$\frac{d\eta}{dt}=\frac{1}{2}z\nu\exp\left[-\frac{U}{k_BT}\right]\left[(1-\eta)^2\exp\left[\frac{(z-1)\eta w_1}{2k_BT}\right]-(1+\eta)^2\exp\left[-\frac{(z-1)\eta w_1}{2k_BT}\right]\right] . \tag{30}$$

By using the identities,

$$(1-\eta)^2=\exp[2\ln(1-\eta)]$$

and

$$\sinh(x)=\frac{\exp(x)-\exp(-x)}{2} ,$$

we can rewrite Eq. (30) as

$$\frac{d\eta}{dt}=z\nu\exp\left[-\frac{U}{k_BT}\right](1-\eta^2)\times\sinh\left[\ln\left[\frac{1-\eta}{1+\eta}\right]+\left[\frac{(z-1)\eta w_1}{2k_BT}\right]\right] . \tag{31}$$

The equilibrium solution is, then, given by

$$T=\frac{(z-1)\eta_e w_1}{2k_B\ln[(1+\eta_e)/(1-\eta_e)]} \tag{32}$$

and the critical temperature

$$T_c=\frac{(z-1)w_1}{4k_B} , \tag{33}$$

which gives a value of $1.75w_1/k_B$ for bcc compared to the value, $1.74w_1/k_B$, obtained from the more elaborate formula (18). The equilibrium long-range-order parameters as a function of time from Eqs. (32) and (22) are plotted together in Fig. 6 which shows that Eq. (32) is a very good approximation of Eq. (22).

In order to understand why the equilibrium states derived from CAM are different from the BW approximation, let us examine the process of atomic exchange and compare the equilibrium solutions (22) and (32). In CAM, the nearest-neighbor pairs have to be considered for the atomic interchange, which is not consistent with the BW approximation in which a single-site is considered. For example, let us consider a case with only nearest-neighbor interactions in a two-dimensional square lattice. In MDT, the atom flux for species A from site 1 to site 2 in Fig. 7 is given by

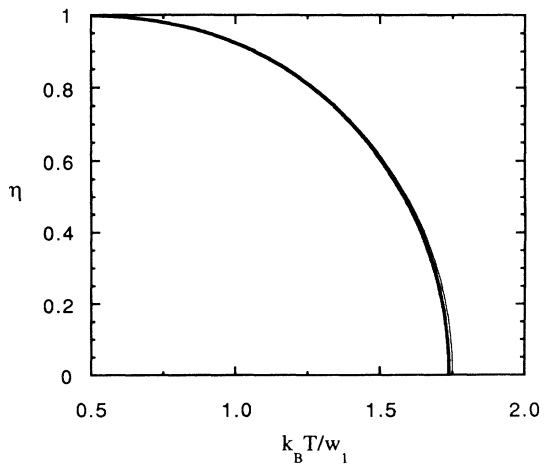

FIG. 6. Long-range-order parameter as a function of temperature. Thick solid line: Eq. (22); thin solid line: Eq. (32).

$$J_{1\to 2}=-L_{1\to 2}\left.\frac{\delta F}{\delta P_A(r)}\right|_{r=2}+L_{2\to 1}\left.\frac{\delta F}{\delta P_A(r)}\right|_{r=1}$$
$$=-L_{1\to 2}\left[\sum_{r'=2+\delta} w_1 P_A(r')+k_B T\ln\left[\frac{P_A(r)}{1-P_A(r)}\right]\right|_{r=2}\Bigg]+L_{2\to 1}\left[\sum_{r'=1+\delta} w_1 P_A(r')+k_B T\ln\left[\frac{P_A(r)}{1-P_A(r)}\right]\right|_{r=1}\Bigg], \tag{34}$$

where $2+\delta$ means the nearest-neighbor sites of site 2 and $1+\delta$ means the nearest-neighbor sites of site 1. In writing the driving force, we do not distinguish the differences between site 1 and sites 4, 6, and 8, which are nearest neighbors of site 2, and between site 2 and sites 3, 5, and 7, which are nearest neighbors of site 1.

On the other hand, in CAM, the flux of atom A from site 1 to site 2 is given by

$$J_{1\to 2}=-\sum_{\{X\}} P_{BA\{X\}}(1,2,\{\mathbf{x}\})R_{BA}(\{X\})$$
$$+\sum_{\{X\}} P_{AB\{X\}}(1,2,\{\mathbf{x}\})R_{AB}(\{X\}), \tag{35}$$

where $\{\mathbf{x}\}$ represents the set of sites 3–8 around the pair 1 and 2. Therefore, the site 1 which is a nearest-neighbor site of 2 is treated differently from the rest nearest-neighbor site 4, 6, and 8. Similarly, the nearest-neighbor site 2 of 1 is treated differently from site 3, 5, and 7. In the evaluation of the rate constants $R_{BA}(\{X\})$ and $R_{AB}(\{X\})$ for the atom exchange, only the bond energies between sites 1 and 3, 1 and 5, 1 and 7, 2 and 4, 2 and 6, and 2 and 8 are considered. Therefore, it is obvious that the transition temperature obtained from CAM in a nearest-neighbor interaction model will be approximately $(z-1)/z$ times the transition temperature obtained from a true single-site mean-field model. In writing Eq. (35), and also Eq. (17), although single-site approximation is employed, some pair correlation information is included, resulting in the equilibrium states, which is close to the Bethe approximation rather than the BW pair approximation. It appears to be also the case in path probability method (PPM) that single-site approximation does not correspond to the BW approximation.[18]

However, for the spin-flip (Glauber) dynamics, the single-site approximation in CAM corresponds exactly to the BW approximation since all the nearest neighbors of the spin-flipping site are treated as the same and the spin-flip occurs at a single-site.

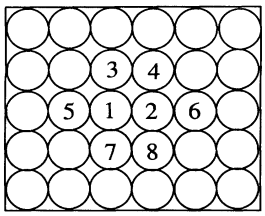

FIG. 7. Schematic diagram showing the exchanging pair and its surrounding influence set of sites in CAM.

If the pair approximation is employed in CAM, the equilibrium states derived are completely consistent with the cluster variation method (CVM) calculation. This is true for both Glauber and Kawasaki dynamics. One may expect any treatment including pair and/or large cluster correlation functions in CAM should reduce the equilibrium states to those calculated by CVM.

The fact that CAM in the single-site approximation for the exchange mechanism does not give rise to the exact BW approximation for the equilibrium thermodynamic states does not invalidate CAM. One has to keep in mind that the BW model itself is an approximation. As a matter of fact, CAM produces a equilibrium states more accurately than the BW model compared to the exact thermodynamic solution. CAM also provides consistent descriptions for the relaxation kinetics of high-order correlation functions in addition to single-site probabilities.

B. The origin for the differences in the kinetics from CAM and MDT

Both the continuum TDGL and C-A kinetic equations and microscopic equations from MDT are based on a free-energy functional, which depends on values of local order parameters in the continuum model or the single-site occupation probabilities in the microscopic model. Both approaches describe the rate changes of order parameters or occupation probabilities with respect to time as linearly proportional to the thermodynamic driving

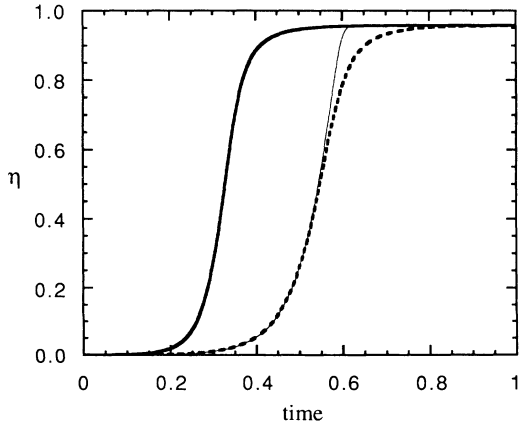

FIG. 8. The temporal evolution of long-range-order parameter as a function of time during ordering at a temperature $T/T_c=0.5$ from Eq. (10) (thin solid line), Eq. (17) (thick solid line), and Eq. (31) (thick dotted line).

force. Therefore, in principle, the description of kinetics by these two approaches are only valid when a system is not too far from the equilibrium state, i.e., the driving force for phase transformation is small. Furthermore, the proportionality constants in both the continuum and microscopic equations are assumed to be independent of the values of the local order parameter or the occupation probabilities. On the other hand, the kinetic equations in CAM based on the master equation method do not assume the existence of free-energy functionals. They do not suffer the approximation that the rate of change of an order parameter is linearly proportional to the thermodynamic driving force.

To make the connections between kinetic equations derived from MDT and those from CAM, let us examine their corresponding kinetic equations (10), (17), and (31). It is noted that Eq. (31) is derived from Eq. (17) with the assumption, $w_1/(2k_BT) \ll 1$. Two points immediately become clear if we compare Eqs. (10), (17), and (31). First, the rate of order parameter change with respect to time is proportional to the driving force in MDT, whereas it is an unknown complex function of driving force in CAM. In the case that the condition $w_1/(2k_BT) \ll 1$ is satisfied, the rate can be written as proportional to sinh(driving force) [Eq. (31)]. Therefore, the linear approximation in MDT is valid only when the driving force is small because of the approximation

$$\sinh(x) = x \ . \tag{36}$$

Second, even when the driving force is small, the proportionality coefficient should not be constant according to Eq. (31). Therefore, to have an accurate prediction about the rate in the small driving force regime, the linear proportionality constant in MDT should be made to be proportional to $(1-\eta^2)$. To have a comparison on the ordering and disordering kinetics, the kinetics obtained from Eqs. (10), (17), and (31) are plotted in Figs. 8, 9, and 10

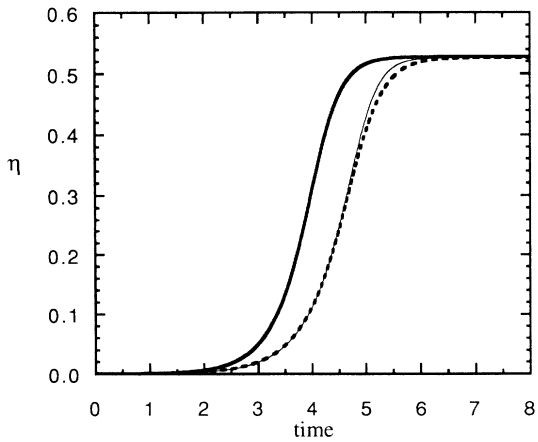

FIG. 9. The temporal evolution of long-range-order parameter as a function of time during ordering at a temperature $T/T_c = 0.9$ from Eq. (10) (thin solid line), Eq. (17) (thick solid line), and Eq. (31) (thick dotted line).

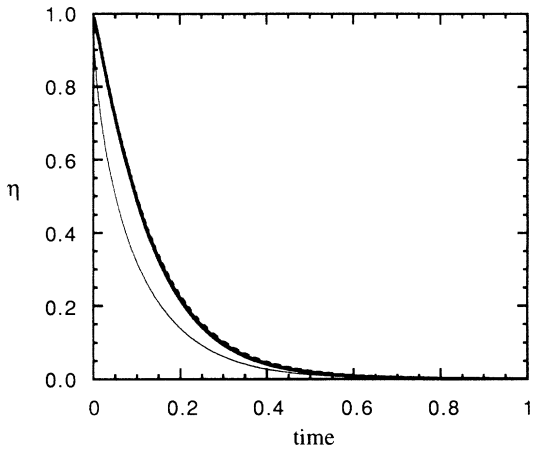

FIG. 10. The temporal evolution of long-range-order parameter as a function of time during ordering at a temperature $T/T_c = 2.0$ from Eq. (10) (thin solid line), Eq. (17) (thick solid line), and Eq. (31) (thick dotted line).

for $T/T_c = 0.5$, 0.9, and 2.0, respectively. It seems that the kinetics predicted from Eq. (10) almost coincides with those from Eq. (31) when the value of long-range-order parameter is small. The ordering kinetics predicted from Eq. (17) is, however, quite different from those predicted by either Eq. (10) or (31) at all values of long-range-order parameter. The difference in kinetics from Eqs. (17) and (31) or (10) decreases when T/T_c increases as expected since the w_1/k_BT decreases as temperature increases.

Ludwig and Park recently compared the kinetics derives from the Langevin-type equations to kinetic Ising models with the thermally activated dynamics using a magnetic spin model.[19] The Langevin-type equations are free-energy-functional-based kinetic equations while the thermally activated dynamics is similar to CAM, but with a kinetic equation similar to Eq. (31) except that the factor $z-1$ is replaced by z. They concluded that, when the driving force is large, there are significant differences in the kinetics described by Langevin equations and kinetic Ising models. The difference can be significantly reduced, however, in the small or intermediate-driving force regime if the proportionality constant is chosen to depend on the instantaneous magnetization $m(t)$ as $[1-m(t)^2]^{1/2}$.

VII. CONCLUSIONS

Long-range-order kinetic equations in binary alloys derived from the cluster-activation method (CAM) and the microscopic diffusion theory (MDT) are examined in the single-site approximation. It is shown that MDT can be derived from CAM in the small driving force regime with small values of long-range parameter. It is demonstrated

that CAM in the single-site approximation produces equilibrium states which are close to the Bethe approximation with the critical temperature for ordering the same as the Bethe approximation, indicating that partial pair correlation information is included in the single-site approximation of CAM. Finally, it is shown that linearized kinetic equations describe reasonably well the disordering kinetics above the order-disorder critical temperature but not the ordering kinetics.

ACKNOWLEDGMENTS

The author is grateful for the financial support from NSF under the Grant No. DMR-9311898 and the partial support from the ARPA/NIST program in mathematical modeling of microstructure evolution in advanced materials. The author would like to thank Dr. J. A. Simmons at NIST and Professor R. Kikuchi at UCLA for useful discussions.

[1]S. Allen and J. W. Cahn, Acta Metall. **27**, 1085 (1979).

[2]For a review, see J. D. Gunton, M. San Miguel, and P. S. Sahni, in *Phase Transitions and Critical Phenomena,* edited by J. Lebowitz (Academic, London, 1983), Vol. 8, p. 267.

[3]L. Q. Chen and A. G. Khachaturyan, Acta Metal. Mater. **39**, 2533 (1991); Phys. Rev. Lett. **70**, 1477 (1993).

[4]A. G. Khachaturyan, Fiz. Tverd. Tela (Leningrad) **9**, 2594 (1967) [Sov. Phys. Solid State **9**, 2040 (1968)].

[5]G. H. Vineyard, Phys. Rev. **102**, 981 (1956).

[6]S. Iida, J. Phys. Soc. Jpn. **10**, 769 (1955).

[7]B. W. Roberts and G. H. Vineyard, J. Appl. Phys. **27**, 203 (1956).

[8]I. I. Kidin and M. A. Shtemel, Fiz. Metal. Metalloved. **11**, 641 (1961).

[9]D. O. Welch, Mater. Sci. Eng. **4**, 9 (1969).

[10]S. Radelaar, J. Phys. Chem. Solids **31**, 219 (1970).

[11]H. Yamauchi and D. de Fontaine, in *Order-Disorder Transformations in Alloys,* edited by H. Warlimont (Springer, Berlin, 1974), p. 148.

[12]C. M. Van Baal, Physica A **111**, 591 (1982); C. M. Van Baal, *ibid.* **113**, 117 (1982); **196**, 116 (1993).

[13]C. M. Van Baal, Physica A **129**, 601 (1985).

[14]L. Anthony and B. Fultz, J. Mater. Res. **4**, 1132 (1989).

[15]B. Fultz, Acta Metal. **37**, 823 (1989); J. Mater. Res. **5**, 1419 (1990).

[16]A. G. Khachaturyan, *Theory of Structural Transformations in Solids* (Wiley, New York, 1983).

[17]H. Yamauchi, Scripta Metal. **7**, 109 (1973).

[18]R. Kikuchi (private communication).

[19]K. F. Ludwig, Jr. and B. Park, Phys. Rev. B **46**, 5079 (1992).